

VISCOUS FRICTION IN SHEARED CONCENTRATED EMULSIONS AND FOAMS

Paper No 69

Authors

Name	E-mail	Institution	Country
DENKOV Nikolai (main author)(speaker)	nd@lcpe.uni-sofia.bg	Sofia University	Bulgaria
TCHOLAKOVA Slavka	sc@lcpe.uni-sofia.bg	University of Sofia	Bulgaria
GOLEMANOV Konstantin		Sofia University	Bulgaria
LIPS Alex		Unilever Global Research Center	United States of America

[Categories]

1.3 Physical Stability. Rheology

Keywords

concentrated emulsions, rheology, theoretical model, jamming, viscous friction

Presentation type :

Contact : nd@lcpe.uni-sofia.bg

Submission date : 2010-03-01 18:28:58

Jury validation date : 2009-12-16 16:17:37

VISCOUS FRICTION IN SHEARED CONCENTRATED EMULSIONS AND FOAMS

Concentrated emulsions, in which the volume fraction of dispersed phase, Φ , is higher than the volume fraction of closely packed spheres, Φ_{CP} , exhibit complex elasto-visco-plastic rheological behavior, controlled by a non-trivial interplay of viscous drag and capillary pressure (1-6). Their rheological properties, under steady shear deformation, are usually described by Herschel-Bulkley model, which includes three parameters - yield stress τ_0 , power-law index n , and consistency, k (1,4,7-10):

$$\tau = \tau_0 + \tau_v = \tau_0 + k\dot{\gamma}^n \quad (1)$$

Here $\dot{\gamma}$ is the applied shear rate, τ is the total shear stress, and τ_v is the rate-depending part of this stress. The dependence of the yield stress, τ_0 , on emulsion characteristics, such as drop size, volume fraction of dispersed phase, and interfacial tension, were studied in detail theoretically and experimentally (1,4,7-10). It was shown that the yield stress of typical emulsions could be presented as a product of the capillary pressure of non-deformed drops and a function, Y , which depends primarily on the volume fraction of the dispersed phase:

$$\tau_0 = (\sigma / R_0)Y(\Phi) \quad (2)$$

Princen (1) found experimentally the following empirical expression for $Y(\Phi)$:

$$Y(\Phi) = \Phi^{1/3}(-0.080 - 0.114\log(1 - \Phi)) \quad (3)$$

which is applicable for polydisperse emulsions. For monodisperse emulsions, Mason et al (10) found

that the following equation is more appropriate for description of the experimental data:

$$\tau_0 = 0.51 \left(\sigma / R_0 \right) (\Phi - 0.62)^2 \quad (4)$$

In recent studies (11-13), we developed a theoretical model for the dependence of τ_v on the shear rate and on the material emulsion characteristics - drop size, volume fraction, and interfacial tension. The basic assumption in this model is that the viscous dissipation occurs predominantly in the thin films, formed between the neighboring drops, which pass by each other dragged by the shear flow, see Fig. 1A. The processes of film formation and thinning were explicitly considered and used to calculate the energy dissipation inside the films. This model predicts power-law index $n \approx 1/2$ and allows one to calculate the consistency, k . Very good agreement was observed between the theoretical predictions and experimental results obtained with foams stabilized by various surfactants (11-13).

The major aim of the current study is to compare the theoretical prediction for τ_0 and τ_v with new experimental results, obtained with concentrated oil-in-water emulsions of mineral and silicone oils, with oil viscosity varied in the range between 3 and 1000 mPa.s.

2/ Theoretical model for viscous friction in concentrated emulsions and foams.

Detailed theoretical model for the viscous friction in steadily sheared foams and concentrated emulsions is described in (11-12). In the current section we present only the main idea of the model and the most important final result which will be used for comparison with the experimental data.

To develop a self-consistent model, we considered idealized sheared emulsion containing monodisperse drops, arranged in face-centred-cubic (fcc) structure. Homogeneous flow with shear rate, $\dot{\gamma}$, corresponds to motion of the neighbouring planes of drops with relative velocity, $u = \dot{\gamma}q$, where q is the plane-to-plane distance, see Figure 1A. To calculate the macroscopic viscous stress in the emulsion, we used a balance of the work performed by the external stress, which drives the emulsion flow, and the energy dissipated inside the emulsion. This balance can be represented in the following form (11-12):

$$\left\langle \dot{E} \right\rangle = \tau_v \dot{\gamma} \quad (5)$$

where τ_v is the viscous stress and $\left\langle \dot{E} \right\rangle$ is the rate of energy dissipation per unit emulsion volume. Note that this relation is equivalent to the law of energy conservation.

Equation (5) converts the problem for calculating the viscous stress, τ_v , into a problem for calculating $\left\langle \dot{E} \right\rangle$. The latter could be solved by considering the possible mechanisms of viscous dissipation of energy, at the structural level of colliding drops. We found (11-12) that the experimental data obtained with various foams could be described by considering two major mechanisms of viscous friction: (1) in the films, formed between two colliding bubbles, and (2) in the surfactant adsorption layers on the bubble surfaces. The second contribution is important for foams with high surface modulus only. For that reason, we consider below only the first mechanism, which is operative in typical concentrated emulsions.

The viscous dissipation of energy in the emulsion films is due to the relative motion of the drops with respect to each other, which leads to the appearance of a local velocity gradient of the fluid confined in the film, see Figure 1B (tangentially immobile drop surfaces are assumed in the entire consideration). Note that no permanent films exist in the flowing emulsion - the emulsion films are formed when the distance between the centres of two colliding drops becomes smaller than the sum of drop radii (11-13), and disappear when the drops are detached from each other, dragged by the flow, see Figure 1A.

To calculate the velocity distribution in the film, and the resulting energy dissipation rate, we considered theoretically the dynamics of the liquid inside the film, by using lubrication

approximation. This consideration showed (12) that the liquid motion inside the film could be decomposed into two “elementary” processes, which occur simultaneously: (1) sliding of the film surfaces, which is due to the relative drop motion and (2) thinning of the film, which is due to the higher dynamic pressure inside the film (imposed by the capillary pressure of the drops, P_C), as compared to the film exterior, see Figure 1B. The numerical estimates showed that the main energy dissipation in the film is due to the sliding motion of the drops (viz. to process 1), however, the film thinning (process 2) should be also considered explicitly, because it determines the film thickness and the resulting velocity gradient inside the film.

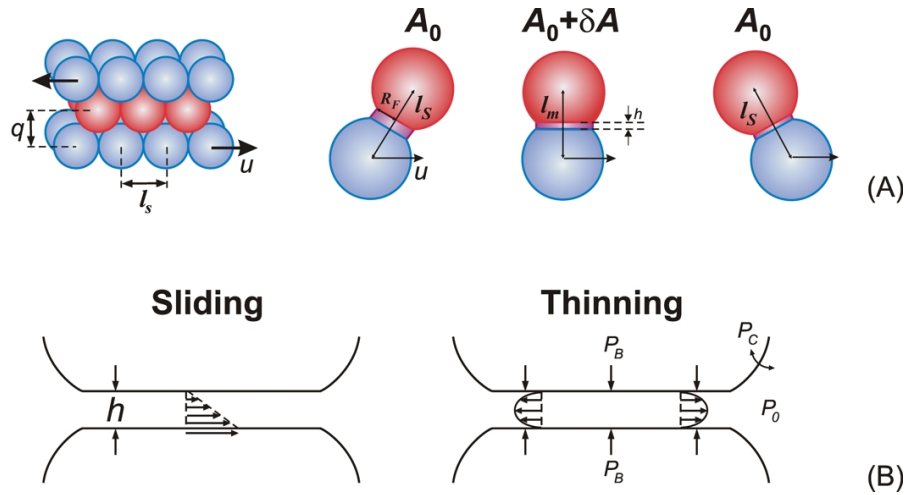


Figure 1. (A) Schematic presentation of the processes of formation, thinning, and disappearance of a planar film between two neighbouring drops in sheared emulsion (11-13). (B) Schematic presentation of the two “elementary” processes determining the film dynamics in sheared emulsions – sliding of the film surfaces (driven by the imposed shear flow) and film thinning (driven by the higher pressure in the drops, P_B , as compared to the pressure in the liquid outside the film, P_0). The viscous dissipation is due predominantly to the sliding motion, while the film thickness (which determines the local shear rate of the liquid in the film and, hence, the rate of viscous dissipation of energy) is governed by the thinning process.

Following the standard hydrodynamic approaches, in (11,12) we calculated the instantaneous film thickness, $h(t)$, and film radius, $R_F(t)$, in the process of drop-drop collision. Next, we calculated the rate of energy dissipation inside the film and the respective energy dissipated during the entire period of existence of one film. Finally, by using Eq. (5), we derived formulas for calculating the viscous stress, in the form of explicit integrals which were solved numerically. The respective numerical results were described very well by the following interpolating formula (12):

$$\overline{\tau}_{VF} \approx 1.16Ca^{0.47} \Phi^{5/6} (\Phi - 0.74)^{0.1} / (1 - \Phi)^{0.5} \quad (6)$$

where $\overline{\tau}_{VF} = \tau_{VF} R_0 / \sigma$ is the dimensionless stress related to the friction in the films, R_0 is drop radius and Φ is oil volume fraction. The subscript “VF” denotes viscous friction inside the films. The model developed in (11,12) showed also that the appropriate mean drop size for description of viscous friction in sheared polydisperse emulsions is the mean volume-surface radius, R_{32} (11,12). Note that Eq. (6) should be used in its range of validity only. The comparison of the model predictions with various experimental data for sheared foams showed that Eq. (6) is applicable at least in the range $0.80 < \Phi < 0.98$ (11,12).

More sophisticated versions of this model were also developed in (13) to account for the possible effects of (1) viscous dissipation of energy in the meniscus region surrounding the films, and

(2) surface forces between the film surfaces. The numerical calculations showed that the energy dissipation in the meniscus region could be neglected in most cases and that the effect of surface forces becomes significant at low shear rates, when the thickness of the dynamic films becomes comparable to the range of surface forces. The latter effect is often important for emulsions, due to the strong dependence of the rate of film thinning on the film diameter. In addition, the theoretical analysis of the effect of attractive surface forces (e.g., of van der Waals or depletion interactions) provided possible mechanistic explanation of the observed “jamming” (liquid-to-solid) transition upon decrease of the shear rate, when the yield stress is reached (14).

3/ Materials and methods.

3/1. Materials. As emulsifier we used the nonionic surfactant polyoxyethylene-8 tridecyl ether (Lutensol A8). The emulsifier concentration in the aqueous solutions (10 wt %) was chosen sufficiently high to suppress drop-drop coalescence during emulsification for all oil volume fractions studied. All aqueous solutions were prepared with deionized water from Milli-Q Organex system (Millipore). As dispersed phase we used several oils of different viscosities: hexadecane with $\eta_D = 3.0$ mPa.s (product of Merck); mineral oil with $\eta_D = 27$ mPa.s (product of Sigma-Aldrich); and three silicone oils with $\eta_D = 95, 194,$ and 1024 mPa.s (denoted for clarity as SilXX, where XX expresses the oil viscosity). The mineral oil and hexadecane were purified from surface-active contaminations by passing them through a glass column, filled with Florisil adsorbent (15). The silicone oils were used as received.

3/2. Emulsification. All emulsions were prepared by using the following procedure: (1) The necessary amount of oil was added to the aqueous phase, under continuous stirring by metal spoon, to form an oil-water premix in the form of coarse emulsion. (2) This premix was homogenized by Ultra Turrax for 5 min, at a specified rotation speed. (3) Samples for measuring the mean drop size and for characterization of the rheological properties of the formed emulsions were taken. The water bath was used for keeping the temperature during emulsification at $T = 25 \pm 3$ °C.

3/3. Rheological properties of the studied emulsions. The rheological properties of the emulsions were determined by the following procedure: (1) Sample from the obtained emulsion was placed between the roughened parallel plates of rheometer. (2) The shear stress was measured as a function of shear rate, which was changed continuously in the range between 1 and 1000 s^{-1} . Two or three consecutive runs were applied for each sample at gap of $400 \mu\text{m}$ to check for the reproducibility of the results. (3) The gap was reduced to $200 \mu\text{m}$ and two additional runs in the same range of shear rates were made. No dependence of the rheological results on the gap width was noticed, which is an indication for absence of wall slip. The experimental data were fitted by the Herschel-Bulkley model and the values of τ_0 , k , and n were determined.

3/4. Determination of drop size distribution. The drop size distribution in the obtained emulsions was determined by video-enhanced optical microscopy (16). For each sample, the diameters of at least 3000 drops were measured. The accuracy of the optical measurements was estimated to be around $0.3 \mu\text{m}$ (16). The mean volume-surface radius, R_{32} , was determined from the measured drop sizes.

4/ Experimental results.

The obtained experimental data for the various emulsions are summarized in Table 1. We compared our experimental results for the measured yield stress with the experimental results obtained by Princen for polydisperse emulsions (eq. (3)) and with the results obtained by Mason for monodisperse emulsions (eq. (4)). From the comparison presented in Figure 2, one sees that most of our data fall between those obtained by Princen (1) and Mason et al. (10). This result could be expected, because the microscopy data showed that our emulsions had intermediate polydispersity in comparison with the emulsions studied in (1) and (10).

Table 1. Mean volume-surface radius, R_{32} , yield stress, τ_0 , consistency, k , and power-law index, n , for emulsions prepared with different oils and having different oil volume fractions. All emulsions are stabilized by 10 wt % A8.

Oil volume fraction, Φ	Oil	R_{32} , μm	τ_0 , Pa	k , $\text{Pa}\cdot\text{s}^n$	n
0.80	Min 27	1.7	17	1.38	0.48 ± 0.02
	Sil 100	2.6	13 ± 2	3.48	0.48 ± 0.02
	Sil 1000	2.4	13 ± 2	3.06	0.59 ± 0.02
0.85	C16	1.5	30 ± 2	3.5	0.45 ± 0.02
	Min27	1.6	28 ± 2	1.8	0.48 ± 0.02
	Sil 100	2.0	30 ± 2	9.5	0.45 ± 0.02
	Sil 1000	1.8	51 ± 2	10.8	0.50 ± 0.02
0.90	Min 27	1.7	66 ± 2	1.7	0.38 ± 0.02
	Sil 100	1.4	77 ± 2	15	0.40 ± 0.02
	Sil 1000	1.2	155 ± 5	20	0.48 ± 0.02

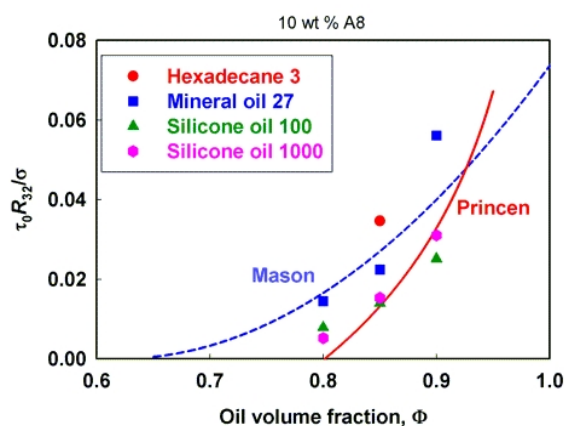


Figure 2. Dimensionless yield stress, $\tau_0 R_{32} / \sigma$, as a function of the oil volume fraction for different emulsions studied (see Table 1 for details). The points are experimental data, the red continuous curve is plotted according to eq. (3) and the blue dashed curve is plotted according to eq. (4).

The obtained experimental data for the dependence of the viscous stress on the shear rate, for emulsions with $\Phi = 0.85$, is shown in Figure 3. One sees that the power-law index for all studied emulsions is around 1/2, which is in a good agreement with the theoretically predicted value (11-12). To compare quantitatively the predictions of eq. (6) with the experimental data for the dependence of the viscous stress on the shear rate, we have measured the values of σ and η_c for the systems studied (accounting also for the depletion of surfactant in the emulsification process).

The comparison between the experimental data and the theoretical equation (6) for the emulsions with volume fraction of 85 % is shown in Figure 3. One sees from this comparison that the theoretical expression describes rather well the experimental data. Similar or slightly worse agreement was observed also at the other volume fractions studied and for the oil of higher viscosity (10000 mPa.s). The complete set of data, with the respective discussion, will be presented in a subsequent paper.

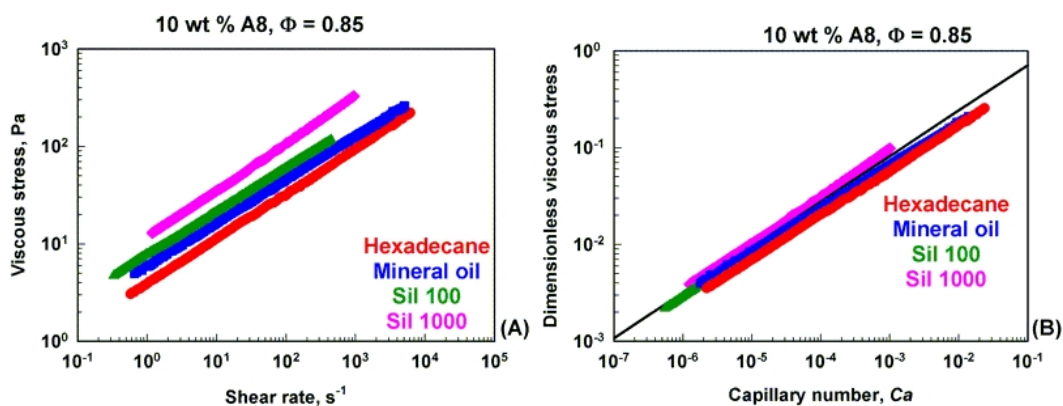


Figure 3. (A) Viscous stress as a function of shear rate for different emulsions with oil volume fraction of 0.85 (see Table 1 for details). (B) Comparison between the experimental data and the predictions of eq. (6). The points are the experimental data from (A), plotted in dimensionless form, whereas the curve is plotted according to eq. (6).

5/ Conclusions.

The theoretical predictions for the yield stress and the viscous stress of steadily sheared emulsions is compared with original experimental data, obtained with concentrated emulsions. The drop volume fraction is varied between 0.8 and 0.9 and the oil viscosity is varied between 3 mPa.s and 10000 mPa.s. Reasonably good agreement between the experimental results and the theoretical predictions is observed, especially for the emulsions of oils with viscosity below 10000 mPa.s.

Acknowledgements. This study was partially funded by project № 202 in “Rila-4” program of the National Science Fund of Bulgaria and it is closely related to the activity of COST P21 Action “Physics of Droplets” of the EU.

References:

1. H.M. Princen, in: Encyclopedia of Emulsion Technology, ed. J. Sjöblom, Marcel Dekker, New York, 2001, p. 243.
2. D. Weaire, Curr. Opin. Colloid Interface Sci., 13 (2008) 171.
3. D. Weaire, W. Drenckhan, Adv. Colloid Interface Sci. 137 (2008) 20.
4. R. Höhler, S. Cohen-Addad, J. Phys: Condens. Matter, 17 (2005) R1041.
5. D. Langevin, ChemPhysChem 9 (2008) 510.
6. A.M. Kraynik, Ann. Rev. Fluid Mech. 20 (1988) 325.
7. H.M. Princen, J. Colloid Interface Sci. 105 (1985) 150.
8. H.M. Princen, A.D. Kiss, J. Colloid Interface Sci. 128 (1989) 176.
9. L. W. Schwartz and H.M. Princen, J. Colloid Interface Sci. 118 (1987) 201.
10. T. G. Mason, J. Bibette, D. A. Weitz, J. Colloid Interface Sci. 179 (1996) 439.
11. N. D. Denkov, S. Tcholakova, K. Golemanov, K.P. Ananth, A. Lips, PRL 100 (2008) 138301.
12. S. Tcholakova, N. D. Denkov, K. Golemanov, K.P. Ananth, A. Lips, PRE 78 (2008) 011405.
13. N. Denkov, S. Tcholakova, K. Golemanov, K. P. Ananth, A. Lips, Soft Matter 7 (2009) 3389.
14. N. D. Denkov, S. Tcholakova, K. Golemanov, A. Lips, Phys. Rev. Letters 103 (2009) 118302.
15. A.G. Gaonkar, R.P. Borwankar, Colloids Surf. 59 (1991) 331.
16. P. S. Denkova, S. Tcholakova, N. D. Denkov, K. D. Danov, B. Campbell, C. Shawl, D. Kim, Langmuir 20 (2004) 11402.